Long-term in vivo integrity and safety of 3D-bioprinted cartilaginous constructs

Received: 28 March 2020 | Revised: 31 May 2020 | Accepted: 23 June 2020

DOI: 10.1002/jbm.b.34687

ORIGINAL RESEARCH REPORT

Society For Biomaterials | WILEY

Long-term in vivo integrity and safety of 3D-bioprinted cartilaginous constructs

Peter Apelgren[1] | Matteo Amoroso[1] | Karin Säljö[1] | Anders Lindahl[2] | Camilla Brantsing[2] | Linnéa Stridh Orrhult[3] | Kajsa Markstedt[3] | Paul Gatenholm[3] | Lars Kölby[1]

[1]Department of Plastic Surgery, Sahlgrenska University Hospital, University of Gothenburg, The Sahlgrenska Academy, Institute of Clinical Sciences, Göteborg, Sweden

[2]Department of Clinical Chemistry and Transfusion Medicine, Institute of Biomedicine, Sahlgrenska University Hospital, Göteborg, Sweden

[3]3D Bioprinting Centre, Department of Chemistry and Chemical Engineering, Chalmers University of Technology, Göteborg, Sweden

Correspondence
Peter Apelgren, Department of Plastic Surgery, Sahlgrenska University Hospital, University of Gothenburg, The Sahlgrenska Academy, Institute of Clinical Sciences, Göteborg, Sweden.
Email: peter.apelgren@gu.se

Funding information
Sahlgrenska University Hospital

Abstract

Long-term stability and biological safety are crucial for translation of 3D-bioprinting technology into clinical applications. Here, we addressed the long-term safety and stability issues associated with 3D-bioprinted constructs comprising a cellulose scaffold and human cells (chondrocytes and stem cells) over a period of 10 months in nude mice. Our findings showed that increasing unconfined compression strength over time significantly improved the mechanical stability of the cell-containing constructs relative to cell-free scaffolds. Additionally, the cell-free constructs exhibited a mean compressive stress and stiffness (compressive modulus) of 0.04 ± 0.05 MPa and 0.14 ± 0.18 MPa, respectively, whereas these values for the cell-containing constructs were 0.11 ± 0.08 MPa (p = .019) and 0.53 ± 0.59 MPa (p = .012), respectively. Moreover, histomorphologic analysis revealed that cartilage formed from the cell-containing constructs harbored an abundance of proliferating chondrocytes in clusters, and after 10 months, resembled native cartilage. Furthermore, extension of the experiment over the complete lifecycle of the animal model revealed no signs of ossification, fibrosis, necrosis, or implant-related tumor development in the 3D-bioprinted constructs. These findings confirm the in vivo biological safety and mechanical stability of 3D-bioprinted cartilaginous tissues and support their potential translation into clinical applications.

KEYWORDS

3D-bioprinting, cartilage, chondrocytes, in vivo, long-term, nude mice

1 | INTRODUCTION

Long-term stability and mechanical resilience are key features of cartilaginous tissue used in reconstructive surgery and that enable their sustainment of configuration/shape and elasticity characteristics. Current methods involve transposing autologous cartilaginous tissue from one site to another in order to reconstruct deformities; however, this technique often leads to significant donor-site morbidity and variable esthetic results (Firmin, 2010; Firmin & Marchac, 2011; Osorno, 1999; Zopf, Iams, Kim, Baker, & Moyer, 2013). Previous studies described methods for creating cartilaginous tissue using three-dimensional (3D)-bioprinting technology and stem cells; however, all of these methods raise concerns regarding the behavior of neocartilage over time in terms of mechanical features and safety (DeForest &

Anseth, 2012; Mouser et al., 2017; You, Eames, & Chen, 2017). For example, cartilage-like tissue can potentially be resorbed, transform into bone, or potentially become carcinogenic (de Vries et al., 2008; Gilbert, O'Connell, Mladenovska, & Dodds, 2018; Hyun, 2010). Therefore, translation of this method to clinical use in humans requires further investigation of its safety and the associated ethical issues (Hyun, 2010).

Native human hyaline cartilage displays several mechanical features that define its physiological function. Compressive stress is related to the ability of tissues to withstand compressive pressure, and in articular cartilage (i.e., hyaline cartilage), this represents the primary function involved in absorbing compressive forces. However, the primary functions of elastic cartilage are defined according to its elasticity and shape-retaining features. In addition to chondrocytes, which constitute ~2% (wet weight) of articular cartilage, mature human cartilage tissue mainly comprises water (up to 80% of its wet weight), collagen, and proteoglycans (Carballo, Nakagawa, Sekiya, & Rodeo, 2017; Sophia Fox, Bedi, & Rodeo, 2009). Chondrocytes originate from mesenchymal stem cells (MSCs), with the addition of MSCs to mixtures of adult chondrocytes enhancing their proliferative capacity via paracrine signaling associated with chondrogenesis that occurs during 3D bioprinting (Apelgren et al., 2017; FDA Public Hearing on Regulation of Stem Cells, 2016; Moller et al., 2017). Given the numerous studies verifying this process, addition of MSCs to promote this activity can be considered the gold standard for 3D-bioprinting technology (Aung, Gupta, Majid, & Varghese, 2011; Bigdeli et al., 2009; de Windt et al., 2014; Grimaud, Heymann, & Redini, 2002; Lettry et al., 2010; Mo et al., 2009; Wu, Leijten, van Blitterswijk, & Karperien, 2013).

Because harvesting MSCs from bone marrow is highly invasive and yields a rather small proportion of stem cells, previous studies evaluated other sources of autologous stem cells. A review by de Windt et al. (de Windt et al., 2014) summarising key studies between 2007 and 2014 noted the use of adipose tissue and, more specifically, a fraction of the lipoaspirate called the stromal vascular fraction (SVF) as sources of stem cells. Compared with MSCs, stem cells derived from the SVF can be more easily harvested in large amounts (e.g., liposuction) and isolated without the need for in vitro culture. Additionally, the SVF contains other types of supporting precursor cells, such as pericytes (Faustini et al., 2010; Jang et al., 2015; Rehman et al., 2004).

Cellulose is a beneficial scaffolding biomaterial, with previous studies confirming its advantageous biocompatibility profile (Pertile et al., 2012; Petersen & Gatenholm, 2011), and the Food and Drug Administration having approved its use in human medical applications. Moreover, cellulose is non-biodegradable and, therefore, promotes retention of the desired shape and mechanical features of 3D-bioprinted constructs over time. Additionally, this characteristic minimizes the release of potentially unfavorable degradation byproducts, thereby ensuring the inert nature of the scaffolding material supporting the autologous cells and precluding an immune response to the graft. A previous study evaluating 3D-bioprinted constructs in mice reported that cellulose implants caused a mild and transient inflammatory response but without any foreign-body response (Pertile et al., 2012). However, although the nude mice used in that study were T cell-deficient, it is possible that the cellulose could have potentially generated a humoral (i.e., B cell-mediated) immune response.

2 | MATERIALS AND METHODS

2.1 | Cell types and culture

Human bone-marrow-derived MSCs originally obtained from female donors (age range: 18–30 years; Rooster Bio, Frederick, MD) were cultured under standard culture conditions (37°C and 5% CO_2) using an MSC high-performance media kit (Rooster Bio).

Human nasoseptal cartilage biopsies were obtained from male donors (age range: 24–40 years; average: 34 ± 5.97 [n = 6]) during routine surgery (i.e., septoplasties or septorhinoplasties) at the Department of Otorhinolaryngology, Head and Neck Surgery, Charité-Medical University (Berlin, Germany). Cartilage harvesting was approved by the University of Berlin Ethics Committee (Dnr EA1/169_12), and all patients provided written informed consent. All cartilage samples were first rinsed in sterile 0.1 M phosphate-buffered saline (PBS) and subsequently in standard culture medium (Dulbecco's modified Eagle medium/F-12 (DMEM; 1:1; Life Technologies, Waltham, MA) supplemented with 10% fetal bovine serum (FBS; HyClone; GE Healthcare, South Logan, UT) and 1% penicillin/streptomycin [P/S; Biochrom, Holliston, MA]) under sterile conditions. Adherent non-cartilaginous tissues, including the perichondrium and epithelium, were removed.

To isolate human primary nasal chondrocytes (hNCs), cartilage samples were sliced into 1 mm × 1 mm pieces, and after discarding the medium, transferred to pronase (Serva, Heidelberg, Germany) digestion solution (10 ml; 20 mg/ml [2%] pronase in DMEM supplemented with 1% P/S without FBS). For the first round of pronase digestion, samples were incubated at 37°C and 5% CO_2 for 45 to 60 min under continuous agitation, after which the pronase solution was discarded, and predigested cartilage samples were washed twice with sterile 1× PBS. For the final digestion, cartilage samples were transferred to collagenase (Gibco; Life Technologies) digestion solution [1 mg/ml (0.1%) collagenase in DMEM complemented with 0.5% FBS and 1% P/S] and incubated for 16 to 18 hr at 37°C and 5% CO_2 with continuous shaking. After centrifugation, total cell number and viability were determined using the Trypan blue exclusion method (Table S1). Subsequently, hNCs were seeded for amplification at an initial density of 5×10^3 cells/cm^2 and cultured in standard culture medium. Upon reaching 80 to 90% confluence, cells were detached, counted (Cell Counter; Thermo Fisher Scientific, Waltham, MA), and cryopreserved to ensure equal treatment of all hNCs harvested from different patients. Cryopreserved hNCs and MSCs were thawed and expanded once in monolayer culture to obtain a sufficient number of cells. Upon reaching 80 to 90% confluence, cells were detached, counted, and resuspended in standard culture medium before mixing with nanofibrillated cellulose/alginate (NFC-A) bioink (CELLINK AB, Gothenburg, Sweden). All experiments were conducted using hNCs and MSCs at passage two.

The SVF was isolated from abdominal lipoaspirate from a female donor according to the protocol described by Zhu et al. (Zhu

et al., 2013). The lipoaspirate was harvested at Art Clinic AB (Gothenburg, Sweden) during an elective cosmetic procedure and processed to extract the SVF after obtaining written consent from the patient. The use of surgical residuals from humans (i.e., lipoaspirate) was approved by the Regional Ethical Committee (Göteborg, Sweden; Dnr 624-16). Briefly, the adipose layer was separated from the lipoaspirate, and the infranatant, containing mostly saline and red blood cells, was discarded. The adipose tissue was then washed with sterile PBS until the adipose layer showed a yellow/gold color, after which it was incubated with an equal volume of sterile 0.075% collagenase 1A (Gibco; Life Technologies) for 30 min at 37°C, during which time the adipose fraction/collagenase mixture was gently swirled every 5 to 10 min to ensure complete digestion. The infranatant containing the SVF was transferred to 50-ml centrifuge tubes, and an equal amount of standard culture medium was added to inactivate the collagenase, followed by centrifugation for 10 min at 1200*g* to collect the SVF as a pellet. Red blood cells were lysed with H_2O for 15 s, followed by the addition of PBS to the samples and centrifugation. The SVF pellet was then resuspended in standard culture medium, and the number of cells was determined before printing. The number of cells added to the bioink was calculated from the living-cell fraction obtained from the cell counter (Table S1).

2.2 | Animals

We used female, nude Balb/C mice (n = 22; 8-weeks old; Scanbur, Karlslunde, Denmark). European husbandry regulations were followed, as were national and local regulations. The study was approved by the Ethical Committee for Animal Experiments at Sahlgrenska University Hospital/Gothenburg University (Göteborg, Sweden; Dnr 36-2016).

2.3 | Bioink and 3D bioprinting

Cells were mixed with NFC-A bioink (CELLINK AB) at a ratio of 1:11, with the initial cell density for all groups at 1×10^6 cells/ml bioink and a cell ratio of 20% hNCs and 80% MSCs or SVF (i.e., SVF-derived stem cells). A 6 mm × 6 mm × 1.2 mm grid was printed using a pneumatic extrusion 3D bioprinter (INKREDIBLE; CELLINK AB) under laminar airflow. Bioprinting pressure in Table S2. After printing, constructs were cross-linked with 100 mM $CaCl_2$ solution for 5 min and washed in standard culture medium, followed by implantation into nude mice within 1 hr after printing. For day 0, printed constructs were directly fixed in 4% paraformaldehyde (PFA) supplemented with 20 mM $CaCl_2$.

2.4 | Experimental design

The animals were divided in three groups: (a) a control group implanted with cell-free constructs, (b) a group implanted with a mixture of hNCs and MSCs, and (c) a group implanted with a mixture of hNCs and SVF (Table 1). For general anaesthesia, each animal received 0.04 ml of the anaesthetic solution (50 mg/ml ketamine and 1 mg/ml medetomidine at a 1:1 ratio) per 20 g body weight via intraperitoneal injection, and the 3D-bioprinted constructs were surgically implanted subcutaneously on the back, followed by closure of the skin pockets with sutures (Vicryl Rapid; Ethicon, Sommerville, NJ, USA). After 8 months and 10 months, respectively, the constructs were harvested, fixed in 4% PFA supplemented with 20 mM $CaCl_2$ overnight at 4°C, and embedded in paraffin. The chosen time frame was determined based on the expected lifespan for this animal model (i.e., 6–12 months) (Anisimov et al., 2001; Brayton, Treuting, & Ward, 2012; Piantanelli et al., 2001).

2.5 | Biomechanical analysis

The mechanical properties of the scaffolds were assessed after printing, as well as after 8 months and 10 months for the implanted constructs, using a universal testing machine (Model 5565A; Instron, Norwood, MA,) equipped with a 10-N load cell and a cylindrical plane-ended stainless-steel indenter (Ø: 12 mm). Unconfined compression tests were performed on wet samples at room temperature. Photographs of the samples before testing were acquired and used to determine the initial dimensions of the samples by measuring the area using ImageJ software (National Institutes of Health, Bethesda, MD). Samples were compressed at intervals of 1% per s (1.08 mm/min) until reaching a 40% compressive strain. Maximum compressive stress at a 40% compressive strain and the tangent modulus at 20 and 30% compressive strain, respectively, were calculated for all samples based on the measured area of each sample.

2.6 | Morphological analysis

The outer millimeter on each side of the sample was discarded, and the paraffinized core sections (5-μm thick) were scanned using a Nikon Eclipse 90i epi-fluorescence microscope equipped with a Nikon DS-Fi2 color head camera (Nikon Instruments, Melville, NY) and the NIS-Elements imaging software suite (v.D4.10.02; Nikon Instruments). Glycosaminoglycan (GAG) production by chondrocytes was visualized with Alcian blue and van Gieson staining, and Safranin-O was used to determine the presence of proteoglycans. Each nucleus surrounded by a blue-stained extracellular matrix was counted manually, with the total

TABLE 1 Experimental design and composition of the 3D constructs

Group	Cell type	Cell composition	8 months (n)	10 months (n)
1	Cell-free	—	3	3
2	Mix 1	20% hNCs, 80% MSCs[a]	4	4
3	**Mix 2**	**20% hNCs, 80% SVF[a]**	**4**	**4**

[a]1×10^6 cells/ml.

number of chondrocytes relative to that in the area of each section determined using PhotoShop (CC 2018, Adobe Systems, San Jose, CA).

2.7 | Statistical analysis

A Mann–Whitney *U* test was used. All statistical calculations were performed using SPSS (v.22.0; IBM Corp., Armonk, NY). A $p < .05$ was considered statistically significant.

3 | RESULTS

3.1 | Scaffolds

The NFC-A scaffolds, both with cells and cell-free blanks, were printed with high levels of printing fidelity and exhibited good printability and dimensional stability. A majority of the cell-containing constructs retained their macroscopic integrity and structural properties and were surgically easy to handle at explantation, whereas the cell-free constructs displayed increased fragility and teared more easily when handled surgically.

3.2 | Animals

In total, 20 of 22 mice survived the entire study period, with one mouse in group 2 dying of unknown cause after 6 months, and another mouse in group 3 requiring premature euthanasia (after 7 months) due to abdominal swelling. Autopsy of the mouse with the abdominal swelling revealed ascites and a prominent hepatosplenomegaly, with histopathologic analysis of tissue samples indicating findings consistent with high-grade lymphoma. Additionally, after ~7 months, some mice exhibited scratch behaviour and eventually developed ulcerations on their backs, which was considered associated with an unspecific skin condition and not grounds to prematurely abort the study. The mice displaying these ulcerations ($n = 5$) were subsequently transferred to the subgroups used for the 8-month time point. During explantation, one animal from this group of transferred mice underwent intraabdominal examination for suspected abdominal swelling, revealing an enlarged spleen and a conspicuous tumor in the left groin, with histopathologic analysis consistent with high-grade lymphoma. The remaining animals ($n = 10$) completed the 10-month experiment without issue.

3.3 | Chondrogenesis and chondrocyte proliferation

In the hNC/MSC group, we measured 140.3 ± 67.4 chondrocytes/mm^2 after 8 months and 87.9 ± 62.7 chondrocytes/mm^2 after 10 months ($p = .30$), whereas in the hNC/SVF group, these values were 59.4 ± 35.6 chondrocytes/mm^2 and 31.7 ± 21.5 chondrocytes/mm^2, respectively ($p = .09$). We observed no significant difference between the two groups at either 8 months or 10 months ($p = .052$ and $p = .2$, respectively), and no chondrocytes were found in the cell-free constructs (Figures 1 to 3).

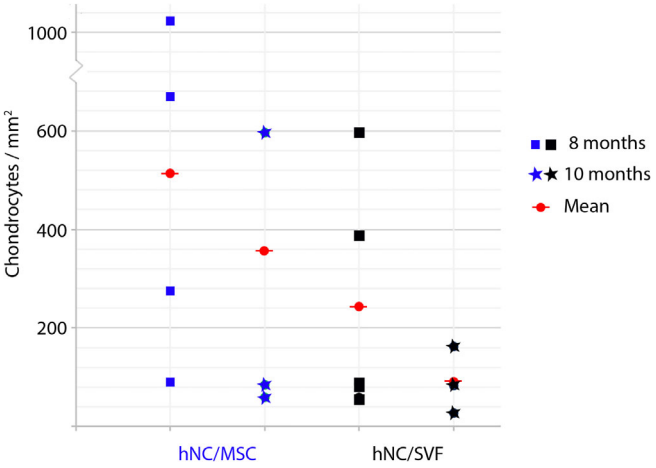

FIGURE 1 Determination of glycosaminoglycan (GAG) production in chondrocytes. The number of GAG-positive chondrocytes after 8 and 10 months, respectively. Although a slight decrease was observed in cell density between the two time points, there was no significant difference between the two stem cell sources (hNC/MSC vs. hNC/SVF)

3.4 | Biomechanical analysis

The implanted scaffolds were prepared for mechanical testing and used for calculation of the cross-section area for each sample. The shape of the samples was uneven and varied (from circular to rectangular), as did the porosity and visible grid structure along with the presence of attached tissue following sample preparation. Additionally, we observed large variations in the measured mechanical properties (compressive stress at 40% strain and compressive modulus at 30% strain). Pooling of the cell-containing constructs and comparison with the cell-free constructs revealed a significant difference in mean compressive stress (cell-free constructs, 0.04 ± 0.05 MPa vs. cell-containing constructs, 0.11 ± 0.08 MPa [$p = .019$]) and stiffness (compressive modulus: 0.14 ± 0.18 MPa vs. 0.53 ± 0.59 MPa, respectively [$p = .012$]) (Figure 4). However, no significant difference was observed between the two different cell-containing groups or between the different time points (Figure S1).

4 | DISCUSSION

Rapid advancements in 3D-bioprinting technology support its eventual clinical application in reconstructive surgery; however, several issues remain unresolved. These include the lack of data concerning the long-term in vivo status of transplanted constructs in order to address safety concerns, such as the risk of ossification, neoplasm

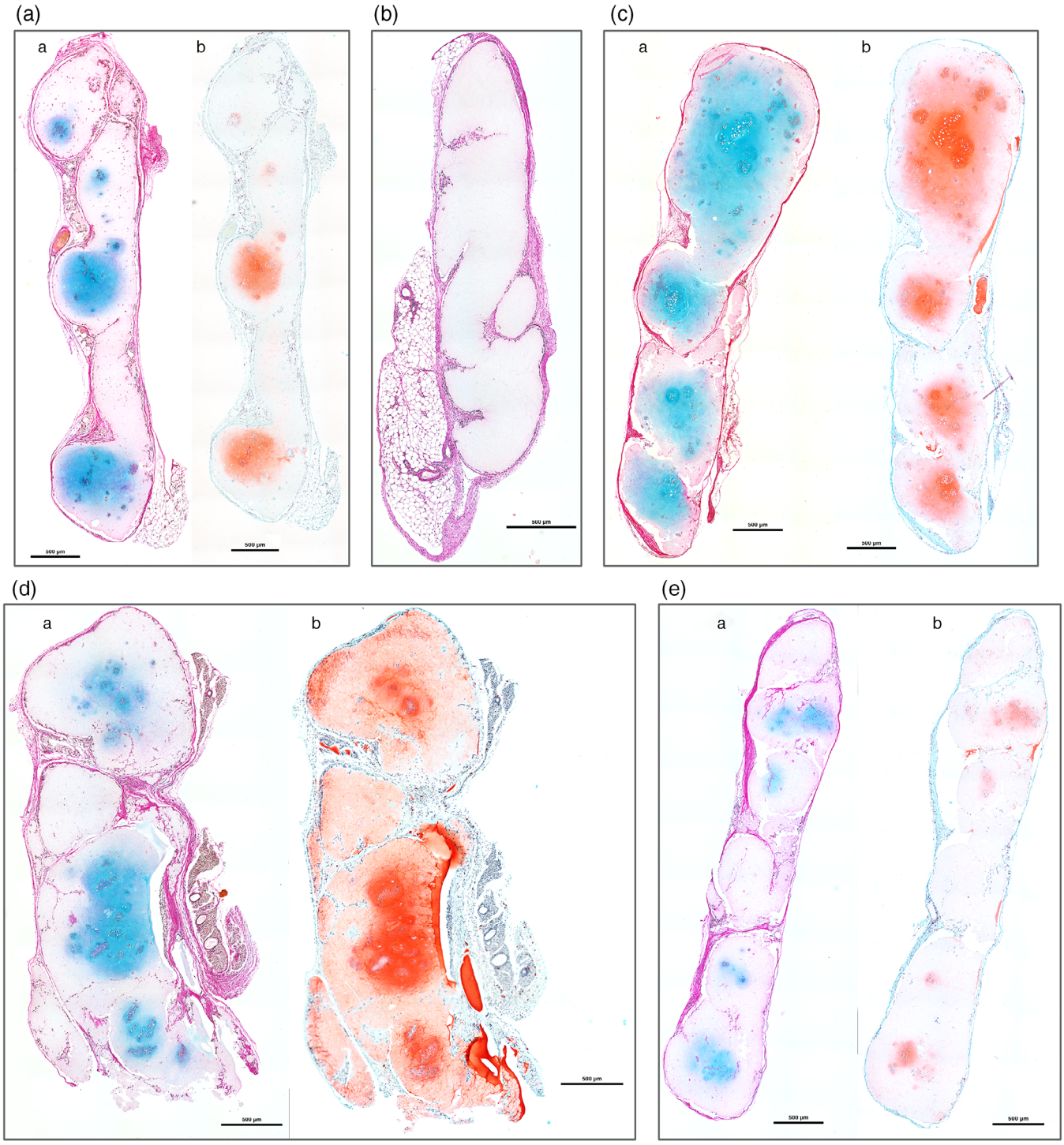

FIGURE 2 Histologic analysis of the three groups. Each group was stained with (a) both Alcian blue and van Gieson and (b) Safranin-O. Mixtures of hNC/MSCs after (a) 8 months and (c) 10 months, respectively. (b) Cell-free construct after 8 months. Mixtures of hNC/SVF after (d) 8 months and (e) 10 months, respectively. Bars = 500 μm

development, and material resilience and shape stability. Additionally, the optimal cell-progenitor composition necessary for chondrogenesis has yet to be established and evaluated.

In this study, we evaluated the long-term outcomes on chondrogenesis associated with transplanted 3D-bioprinted constructs, with the results suggesting that constructs containing cells were more stable over time. Moreover, we observed survival and proliferation of the transplanted human chondrocytes accompanied by formation of cartilage-like tissues, with their survival limited only by the longevity of the animal model used. Furthermore, over the 10-month study

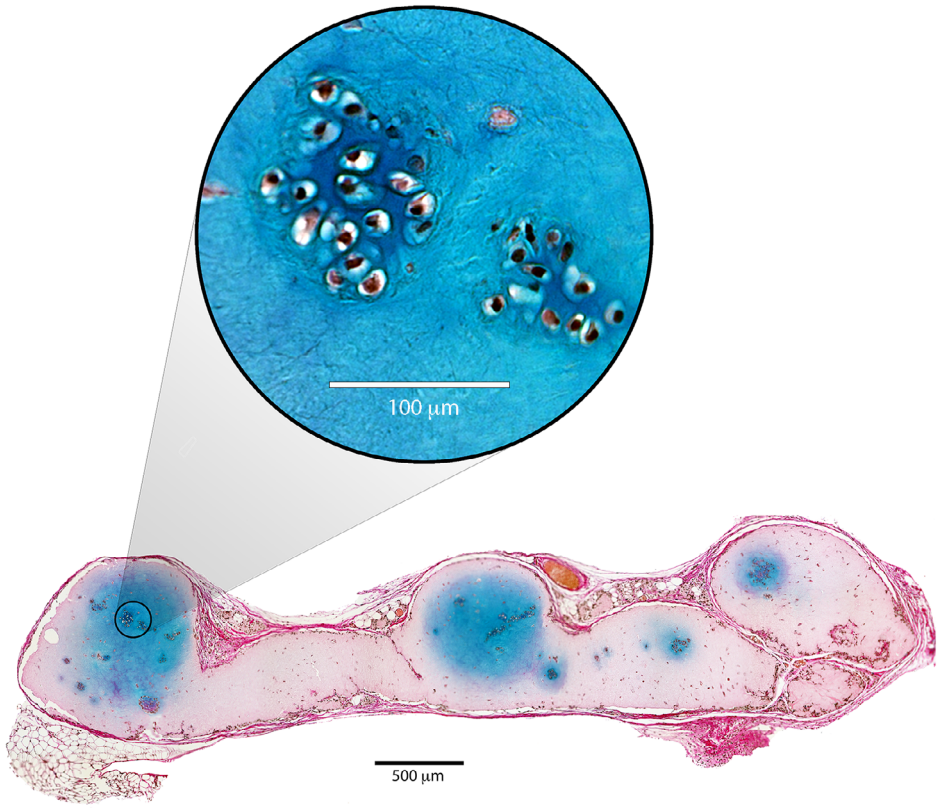

FIGURE 3 Histological section from the hNC/MSC group after 8 months. Bar = 500 μm. Magnification shows two chondrocyte clusters (bar = 100 μm)

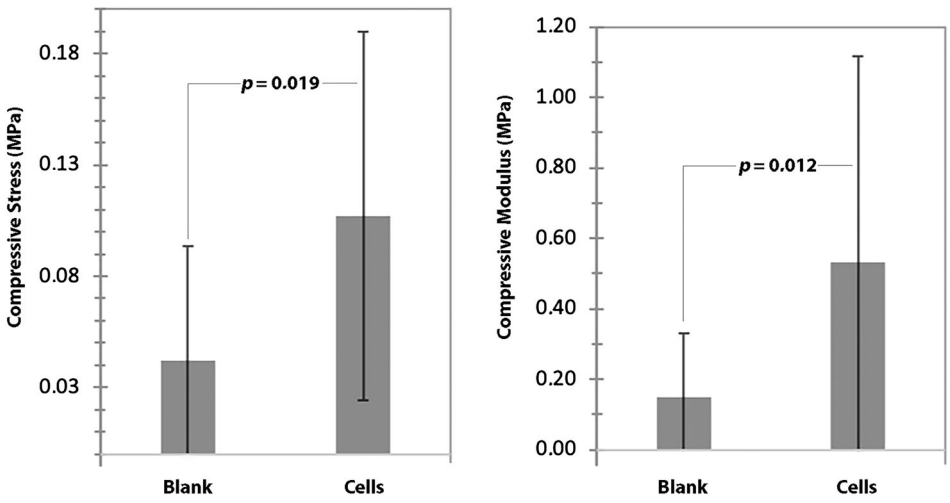

FIGURE 4 Comparison of cell-free constructs with cell-containing constructs (hNC/MSC vs. hNC/SVF). Compressive stress at 40% strain (*left*) and compressive modulus (stiffness) at 30% strain (*right*)

period, we observed no adverse events, such as neoplasms, ossification, or necrosis.

Mechanical assessment of the constructs revealed that the cell-containing constructs exhibited greater resilience and robustness over time relative to the cell-free constructs. Measurement of compressive stress allows determination of the force required to deform a sample to a certain percentage (at 40% strain, the sample is compressed to 40% of its initial height), whereas measurement of stiffness (modulus) indicates how well a sample resists elastic deformation while being compressed. Mechanical testing over the 8- and 10-month evaluation of the 3D-bioprinted grids following implantation is challenging, as the grid dimensions vary between samples due to their lack of homogeneity, with this primarily concerning the variable content of connective tissue stuck to the grids, which in turn influences mechanical properties and results in large variance in the measurements. Our findings indicated that the mechanical properties of the constructs were comparable with native human cartilage. The mechanical data were comparable to findings reported previously regarding cell-free samples prepared with similar scaffold material (cellulose and alginate) (compressive stress at 30% strain: 0.032 ± 0.005 MPa; and compressive stiffness at 30% strain: 0.15 ± 0.05 MPa) (Markstedt et al., 2015; Nimeskern et al., 2013).

After 10 months, we observed a large population of viable chondrocytes, with the overall chondrocyte cell count and clustering in the hNC/MSC and hNC/SVF constructs indicating similarities with those of native cartilage. In mature human cartilage, the number of chondrocytes in weight-bearing, hyaline cartilage is ~90 chondrocytes/mm^2, with this number declining rapidly with age (Bobacz, Erlacher, Smolen, Soleiman, & Graninger, 2004). The mean cell count in the present study was ~100 chondrocytes/mm^2 at 8 months and ~ 60 chondrocytes/mm^2 at 10 months, suggesting an age-related decline in our model. Moreover, histologic analysis confirmed the presence of features in the 3D-bioprined cartilage resembling those of human cartilage. Based on the results from a previous study using FISH analysis, the proliferating chondrocytes originates from the adult chondrocytes, and not from the stem cells (Apelgren et al., 2017).

Our results indicated that SVF-derived stem cells exerted quantitatively similar trophic effects on chondrocyte proliferation to those observed using bone-marrow-derived MSCs. Specifically, we found no significant difference in chondrogenesis between either of the two cell-containing groups or the 8- and 10-month subgroups, regardless of stem cell source. Previous studies reported the capacity of MSCs to enhance chondrogenesis (Apelgren et al., 2017; Moller et al., 2017), and Wu et al. (Wu et al., 2016) indicated that stem cells derived from the SVF of adipose tissue showed and even greater capacity for promoting chodrogenesis relative to that of MSCs (Wu et al., 2016). From a clinical standpoint, the SVF is highly relevant because of the relative ease associated with its harvesting process and the large amount of stem cells that can be retrieved. Furthermore, the SVF does not require in vitro manipulation or expansion prior to transplantation, which potentially increases the ease of regulatory approval of the entire procedure associated with autologous transplantation. We used the specific 20/80 ratio (hNC/MSCs and hNC/SVF, respectively) as it is well established to be an optimal ratio for induction of cartilage regeneration (de Windt et al., 2014; Leijten et al., 2013; Martinez Avila et al., 2015; Wu et al., 2011; Wu, Prins, Helder, van Blitterswijk, & Karperien, 2012; Zuo et al., 2013).

The cell count and mechanical data showed that both hNC/MSCs and hNC/SVF promoted the in vivo formation of similar native-like cartilaginous tissue after 8 months. Further studies are required to further discriminate MSCs from SVF-derived stem cells with regard to how rapidly they create cartilage-like tissues. Because the SVF, similar to adipose stem cells, contains intrinsic growth factors (e.g., pericytes and other angiogenic building blocks) that surround cartilaginous tissue and promote its proliferation (Rehman et al., 2004; Rubina et al., 2009), use of an hNC/SVF mixture might represent a faster method for cartilage regeneration.

Additionally, we histologically evaluated the conceivable transition to bone on the part of the two stem cell subsets, finding no indication of bone-tissue formation. The endochondral pathway involved in bone formation uses chondrocytes as primary precursor cells but requires systemic, as well as local, stimuli (growth factors), to activate the necessary transcription factors. When activated at bone-forming sites, chondrocytes withdraw, and vascularisation of the cartilage extracellular matrix occurs accompanied by increases in osteocyte and bone-marrow cell populations (Mackie, Ahmed, Tatarczuch, Chen, & Mirams, 2008). In the present study, perseverance of the newly formed cartilage tissue might be attributable to the lack of paracrine signaling and trophic influence that trigger bone formation via the endochondral pathway, thereby allowing the 3D-bioprinted structures to retain their cartilaginous features (i.e., elasticity) over time.

Two mice in the hNC/SVF group exhibited tumors histopathologically resembling lymphoreticular neoplasms and, therefore, unrelated to the chondrocyte lineage. According to previous studies, aging nude mice are commonly afflicted by spontaneous lymphoreticular cancers (Anisimov, 1987; Anisimov et al., 2001; Brayton et al., 2012; Bronson & Lipman, 1993; Frith, 1983; Sharkey & Fogh, 1979; Storer, 1966). Importantly, we found no neoplasms, such as sarcomas, conceivably correlated with transplant of the 3D-bioprinted constructs.

Our study has limitations. Specifically, the lifespan of the animal model used for in vivo evaluation is estimated at ~12 months; therefore, all the animals used in this study were close to this threshold toward the end of our experimental assessment and exhibiting an overall decline in physiological capability and resilience. Although not significant, we observed declines in chondrocyte proliferation according to cell count, which might have been associated with the physiological limitations of the animal model rather than the transplanted constructs. Future studies should focus on the use of animal models providing a longer lifespan. Another major limitation of the present study is the small number of animals in each group, resulting in low statistical power and difficulties to detect differences.

5 | CONCLUSIONS

This study showed that the 3D-bioprinted constructs containing chondrocytes and stem cells effectively created viable and mechanically stable cartilage-like tissues over a 10-month period in a mouse model. Importantly, we observed no adverse effects following transplantation, such as engraftment-related neoplasms, ossification, or necrosis, over the lifespan of the animals. These results confirmed the clinical efficacy of 3D-bioprinting technology and encourage further trials using immunocompetent animal models (e.g., pigs) and humans.

ACKNOWLEDGMENTS

The authors thank the staff at Art Clinic AB for providing the lipoaspirate used in this study. Additionally, we are grateful to Johan Mölne, MD, PhD, senior consultant pathologist at Sahlgrenska University Hospital, for help with histopathologic analyses. Furthermore, the cartilage samples have been kindly provided by Dr. Katharina Stölzel at the Department of Otorhinolaryngology, Head and Neck Surgery at Charité Universitätsmedizin, Campus Charité Mitte in Berlin, Germany. We would also like to acknowledge Dr. Silke Schwarz and Prof. Dr. Gundula Schulze-Tanzil at the Department of Anatomy at Paracelsus Medical University in Nürnberg, Germany, who performed the cell isolation and cultivation procedures.

CONFLICT OF INTEREST

The authors have no conflicts of interest to declare.

ORCID

Peter Apelgren https://orcid.org/0000-0003-0451-7771

REFERENCES

Anisimov, V. N. (1987). Life span and tumor incidence in animals of various species. *Eksp Onkol*, *9*(5), 17–23 60.

Anisimov, V. N., Zabezhinski, M. A., Rossolini, G., Zaia, A., Piantanelli, A., Basso, A., & Piantanelli, L. (2001). Long-live euthymic BALB/c-nu mice. II: Spontaneous tumors and other pathologies. *Mechanisms of Ageing and Development*, *122*(5), 477–489.

Apelgren, P., Amoroso, M., Lindahl, A., Brantsing, C., Rotter, N., Gatenholm, P., & Kölby, L. (2017). Chondrocytes and stem cells in 3D-bioprinted structures create human cartilage in vivo. *PLoS One*, *12*(12), e0189428.

Aung, A., Gupta, G., Majid, G., & Varghese, S. (2011). Osteoarthritic chondrocyte-secreted morphogens induce chondrogenic differentiation of human mesenchymal stem cells. *Arthritis and Rheumatism*, *63*(1), 148–158.

Bigdeli, N., Karlsson, C., Strehl, R., Concaro, S., Hyllner, J., & Lindahl, A. (2009). Coculture of human embryonic stem cells and human articular chondrocytes results in significantly altered phenotype and improved chondrogenic differentiation. *Stem Cells*, *27*(8), 1812–1821.

Bobacz, K., Erlacher, L., Smolen, J., Soleiman, A., & Graninger, W. B. (2004). Chondrocyte number and proteoglycan synthesis in the aging and osteoarthritic human articular cartilage. *Annals of the Rheumatic Diseases*, *63*(12), 1618–1622.

Brayton, C. F., Treuting, P. M., & Ward, J. M. (2012). Pathobiology of aging mice and GEM: Background strains and experimental design. *Veterinary Pathology*, *49*(1), 85–105.

Bronson, R. T., & Lipman, R. D. (1993). FRAR course on laboratory approaches to aging. The role of pathology in rodent experimental gerontology. *Aging (Milano)*, *5*(4), 253–257.

Carballo, C. B., Nakagawa, Y., Sekiya, I., & Rodeo, S. A. (2017). Basic science of articular cartilage. *Clinics in Sports Medicine*, *36*(3), 413–425.

de Vries, R. B., Oerlemans, A., Trommelmans, L., Dierickx, K., & Gordijn, B. (2008). Ethical aspects of tissue engineering: A review. *Tissue Engineering. Part B, Reviews*, *14*(4), 367–375.

de Windt, T. S., Hendriks, J. A. A., Zhao, X., Vonk, L. A., Creemers, L. B., Dhert, W. J. A., … Saris, D. B. F. (2014). Concise review: Unraveling stem cell cocultures in regenerative medicine: Which cell interactions steer cartilage regeneration and how? *Stem Cells Translational Medicine*, *3*(6), 723–733.

DeForest, C. A., & Anseth, K. S. (2012). Advances in bioactive hydrogels to probe and direct cell fate. *Annual Review of Chemical and Biomolecular Engineering*, *3*, 421–444.

Faustini, M., Bucco, M., Chlapanidas, T., Lucconi, G., Marazzi, M., Tosca, M. C., … Torre, M. L. (2010). Nonexpanded mesenchymal stem cells for regenerative medicine: Yield in stromal vascular fraction from adipose tissues. *Tissue Engineering. Part C, Methods*, *16*(6), 1515–1521.

FDA Public Hearing on Regulation of Stem Cells. 2016.

Firmin, F. (2010). State-of-the-art autogenous ear reconstruction in cases of microtia. *Advances in Oto-Rhino-Laryngology*, *68*, 25–52.

Firmin, F., & Marchac, A. (2011). A novel algorithm for autologous ear reconstruction. *Seminars in Plastic Surgery*, *25*(4), 257–264.

Frith, C. H. (1983). Incidence of hepatic metastases for various neoplasms in several strains of mice. *Toxicologic Pathology*, *11*(2), 120–128.

Gilbert, F., O'Connell, C. D., Mladenovska, T., & Dodds, S. (2018). Print me an organ? Ethical and regulatory issues emerging from 3D bioprinting in medicine. *Science and Engineering Ethics*, *24*(1), 73–91.

Grimaud, E., Heymann, D., & Redini, F. (2002). Recent advances in TGF-beta effects on chondrocyte metabolism. Potential therapeutic roles of TGF-beta in cartilage disorders. *Cytokine & Growth Factor Reviews*, *13*(3), 241–257.

Hyun, I. (2010). The bioethics of stem cell research and therapy. *The Journal of Clinical Investigation*, *120*(1), 71–75.

Jang, Y., Koh, Y. G., Choi, Y. J., Kim, S. H., Yoon, D. S., Lee, M., & Lee, J. W. (2015). Characterization of adipose tissue-derived stromal vascular fraction for clinical application to cartilage regeneration. *In Vitro Cellular & Developmental Biology. Animal*, *51*(2), 142–150.

Leijten, J. C., Georgi, N., Wu, L., van Blitterswijk, C. A., & Karperien, M. (2013). Cell sources for articular cartilage repair strategies: Shifting from monocultures to cocultures. *Tissue Engineering. Part B, Reviews*, *19*(1), 31–40.

Lettry, V., Hosoya, K., Takagi, S., & Okumura, M. (2010). Coculture of equine mesenchymal stem cells and mature equine articular chondrocytes results in improved chondrogenic differentiation of the stem cells. *The Japanese Journal of Veterinary Research*, *58*(1), 5–15.

Mackie, E. J., Ahmed, Y. A., Tatarczuch, L., Chen, K. S., & Mirams, M. (2008). Endochondral ossification: How cartilage is converted into bone in the developing skeleton. *The International Journal of Biochemistry & Cell Biology*, *40*(1), 46–62.

Markstedt, K., Mantas, A., Tournier, I., Martinez Avila, H., Hagg, D., & Gatenholm, P. (2015). 3D bioprinting human chondrocytes with Nanocellulose-alginate bioink for cartilage tissue engineering applications. *Biomacromolecules*, *16*(5), 1489–1496.

Martinez Avila, H., Feldman, E. M., Pleumeekers, M. M., Nimeskern, L., Kuo, W., de Jong, W. C., & Gatenholm, P. (2015). Novel bilayer bacterial nanocellulose scaffold supports neocartilage formation in vitro and in vivo. *Biomaterials*, *44*, 122–133.

Mo, X. T., Guo, S. C., Xie, H. Q., Deng, L., Zhi, W., Xiang, Z., … Yang, Z. M. (2009). Variations in the ratios of co-cultured mesenchymal stem cells and chondrocytes regulate the expression of cartilaginous and osseous phenotype in alginate constructs. *Bone*, *45*(1), 42–51.

Moller, T., Amoroso, M., Hagg, D., Brantsing, C., Rotter, N., Apelgren, P., … Gatenholm, P. (2017). In vivo Chondrogenesis in 3D bioprinted human cell-laden hydrogel constructs. *Plastic and Reconstructive Surgery. Global Open*, *5*(2), e1227.

Mouser, V. H. M., Levato, R., Bonassar, L. J., D'Lima, D. D., Grande, D. A., Klein, T. J., … Malda, J. (2017). Three-dimensional bioprinting and its potential in the field of articular cartilage regeneration. *Cartilage*, *8*(4), 327–340.

Nimeskern, L., Martínez Ávila, H., Sundberg, J., Gatenholm, P., Müller, R., & Stok, K. S. (2013). Mechanical evaluation of bacterial nanocellulose as an implant material for ear cartilage replacement. *Journal of the Mechanical Behavior of Biomedical Materials*, *22*, 12–21.

Osorno, G. (1999). Autogenous rib cartilage reconstruction of congenital ear defects: Report of 110 cases with Brent's technique. *Plastic and Reconstructive Surgery*, *104*(7), 1951–1962 discussion 1963-4.

Pertile, R. A., Moreira, S., Gil da Costa, R. M., Correira, A., Guardao, L., Gartner, F., … & Gama, M. (2012). Bacterial cellulose: Long-term biocompatibility studies. *Journal of Biomaterials Science. Polymer Edition*, *23*(10), 1339–1354.

Petersen, N., & Gatenholm, P. (2011). Bacterial cellulose-based materials and medical devices: Current state and perspectives. *Applied Microbiology and Biotechnology*, *91*(5), 1277–1286.

Piantanelli, L., Zaia, A., Rossolini, G., Piantanelli, A., Basso, A., & Anisimov, V. N. (2001). Long-live euthymic BALB/c-nu mice. I. Survival study suggests body weight as a life span predictor. *Mechanisms of Ageing and Development*, *122*(5), 463–475.

Rehman, J., Traktuev, D., Li, J., Merfeld-Clauss, S., Temm-Grove, C. J., Bovenkerk, J. E., … March, K. L. (2004). Secretion of angiogenic and antiapoptotic factors by human adipose stromal cells. *Circulation*, *109*(10), 1292–1298.

Rubina, K., Kalinina, N., Efimenko, A., Lopatina, T., Melikhova, V., Tsokolaeva, Z., … Parfyonova, Y. (2009). Adipose stromal cells stimulate angiogenesis via promoting progenitor cell differentiation, secretion of angiogenic factors, and enhancing vessel maturation. *Tissue Engineering. Part A*, *15*(8), 2039–2050.

Sharkey, F. E., & Fogh, J. (1979). Incidence and pathological features of spontaneous tumors in athymic nude mice. *Cancer Research*, *39*(3), 833–839.

Sophia Fox, A. J., Bedi, A., & Rodeo, S. A. (2009). The basic science of articular cartilage: Structure, composition, and function. *Sports Health*, *1*(6), 461–468.

Storer, J. B. (1966). Longevity and gross pathology at death in 22 inbred mouse strains. *Journal of Gerontology*, *21*(3), 404–409.

Wu, L., Leijten, J., van Blitterswijk, C. A., & Karperien, M. (2013). Fibroblast growth factor-1 is a mesenchymal stromal cell-secreted factor stimulating proliferation of osteoarthritic chondrocytes in co-culture. *Stem Cells and Development*, *22*(17), 2356–2367.

Wu, L., Leijten, J. C. H., Georgi, N., Post, J. N., van Blitterswijk, C. A., & Karperien, M. (2011). Trophic effects of mesenchymal stem cells increase chondrocyte proliferation and matrix formation. *Tissue Engineering. Part A*, *17*(9–10), 1425–1436.

Wu, L., Prins, H. J., Helder, M. N., van Blitterswijk, C. A., & Karperien, M. (2012). Trophic effects of mesenchymal stem cells in chondrocyte co-cultures are independent of culture conditions and cell sources. *Tissue Engineering. Part A*, *18*(15–16), 1542–1551.

Wu, L., Prins, H. J., Leijten, J., Helder, M. N., Evseenko, D., Moroni, L., … Karperien, M. (2016). Chondrocytes Cocultured with stromal vascular fraction of adipose tissue present more intense Chondrogenic characteristics than with adipose stem cells. *Tissue Engineering. Part A*, *22*(3–4), 336–348.

You, F., Eames, B. F., & Chen, X. (2017). Application of extrusion-based hydrogel bioprinting for cartilage tissue engineering. *International Journal of Molecular Sciences*, *18*(7), Article no 1597.

Zhu, M., Heydarkhan-Hagvall, S., Hedrick, S., Benhaim, P., & Zuk, P. (2013). Manual isolation of adipose-derived stem cells from human lipoaspirates. *Journal of Visualized Experiments*, (79), e50585.

Zopf, D. A., Iams, W., Kim, J. C., Baker, S. R., & Moyer, J. S. (2013). Full-thickness skin graft overlying a separately harvested auricular cartilage graft for nasal alar reconstruction. *JAMA Facial Plastic Surgery*, *15*(2), 131–134.

Zuo, Q., Cui, W., Liu, F., Wang, Q., Chen, Z., & Fan, W. (2013). Co-cultivated mesenchymal stem cells support chondrocytic differentiation of articular chondrocytes. *International Orthopaedics*, *37*(4), 747–752.

SUPPORTING INFORMATION

Additional supporting information may be found online in the Supporting Information section at the end of this article.

How to cite this article: Apelgren P, Amoroso M, Säljö K, et al. Long-term in vivo integrity and safety of 3D-bioprinted cartilaginous constructs. *J Biomed Mater Res*. 2021;109: 128–136. https://doi.org/10.1002/jbm.b.34687